

**Luminex**  
complexity simplified.



**Flow Cytometry with Vision.**

Amnis<sup>®</sup> ImageStream<sup>™</sup> Mk II and  
FlowSight<sup>™</sup> Imaging Flow Cytometers

**LEARN MORE >**



## Phenotypic Variation in Aicardi–Goutières Syndrome Explained by Cell-Specific IFN-Stimulated Gene Response and Cytokine Release

This information is current as of November 25, 2020.

Eloy Cuadrado, Iliana Michailidou, Emma J. van Bodegraven, Machiel H. Jansen, Jacqueline A. Sluijs, Dirk Geerts, Pierre-Olivier Couraud, Lidia De Filippis, Angelo L. Vescovi, Taco W. Kuijpers and Elly M. Hol

*J Immunol* 2015; 194:3623-3633; Prepublished online 13 March 2015;  
doi: 10.4049/jimmunol.1401334  
<http://www.jimmunol.org/content/194/8/3623>

**Supplementary Material** <http://www.jimmunol.org/content/suppl/2015/03/13/jimmunol.1401334.DCSupplemental>

**References** This article **cites 47 articles**, 13 of which you can access for free at:  
<http://www.jimmunol.org/content/194/8/3623.full#ref-list-1>

**Why *The JI*? Submit online.**

- **Rapid Reviews! 30 days\*** from submission to initial decision
- **No Triage!** Every submission reviewed by practicing scientists
- **Fast Publication!** 4 weeks from acceptance to publication

*\*average*

**Subscription** Information about subscribing to *The Journal of Immunology* is online at:  
<http://jimmunol.org/subscription>

**Permissions** Submit copyright permission requests at:  
<http://www.aai.org/About/Publications/JI/copyright.html>

**Email Alerts** Receive free email-alerts when new articles cite this article. Sign up at:  
<http://jimmunol.org/alerts>

*The Journal of Immunology* is published twice each month by  
The American Association of Immunologists, Inc.,  
1451 Rockville Pike, Suite 650, Rockville, MD 20852  
Copyright © 2015 by The American Association of  
Immunologists, Inc. All rights reserved.  
Print ISSN: 0022-1767 Online ISSN: 1550-6606.



# Phenotypic Variation in Aicardi–Goutières Syndrome Explained by Cell-Specific IFN-Stimulated Gene Response and Cytokine Release

Eloy Cuadrado,<sup>\*,†</sup> Iliana Michailidou,<sup>\*,‡,1</sup> Emma J. van Bodegraven,<sup>§,1</sup> Machiel H. Jansen,<sup>†</sup> Jacqueline A. Sluijs,<sup>\*,§</sup> Dirk Geerts,<sup>¶</sup> Pierre-Olivier Couraud,<sup>||</sup> Lidia De Filippis,<sup>#</sup> Angelo L. Vescovi,<sup>#</sup> Taco W. Kuijpers,<sup>†</sup> and Elly M. Hol<sup>\*,§,\*\*\*</sup>

Aicardi–Goutières syndrome (AGS) is a monogenic inflammatory encephalopathy caused by mutations in *TREX1*, *RNASEH2A*, *RNASEH2B*, *RNASEH2C*, *SAMHD1*, *ADARI*, or *MDA5*. Mutations in those genes affect normal RNA/DNA intracellular metabolism and detection, triggering an autoimmune response with an increase in cerebral IFN- $\alpha$  production by astrocytes. Microangiopathy and vascular disease also contribute to the neuropathology in AGS. In this study, we report that AGS gene silencing of *TREX1*, *SAMHD1*, *RNASEH2A*, and *ADARI* by short hairpin RNAs in human neural stem cell–derived astrocytes, human primary astrocytes, and brain-derived endothelial cells leads to an antiviral status of these cells compared with nontarget short hairpin RNA–treated cells. We observed a distinct activation of the IFN-stimulated gene signature with a substantial increase in the release of proinflammatory cytokines (IL-6) and chemokines (CXCL10 and CCL5). A differential impact of AGS gene silencing was noted; silencing *TREX1* gave rise to the most dramatic in both cell types. Our findings fit well with the observation that patients carrying mutations in *TREX1* experience an earlier onset and fatal outcome. We provide in the present study, to our knowledge for the first time, insight into how astrocytic and endothelial activation of antiviral status may differentially lead to cerebral pathology, suggesting a rational link between proinflammatory mediators and disease severity in AGS. *The Journal of Immunology*, 2015, 194: 3623–3633.

**A** icardi–Goutières syndrome (AGS; MIM 225750) is a genetically determined neuroinflammatory disorder that typically becomes apparent in infancy (1). AGS encephalopathy is characterized by basal-ganglia calcification, white matter abnormalities, and a chronic cerebrospinal fluid (CSF) lymphocytosis. Patients with AGS suffer from microcephaly, spasticity, dys-

tonia, psychomotor retardation, and have a 25% chance of early childhood death (2). AGS is monogenic but genetically heterogeneous. It can result from mutations in the DNA exonuclease *TREX1* (3), the three nonallelic components of the RNase H2 endonuclease complex (*RNASEH2B*, *RNASEH2C*, and *RNASEH2A*) (4), the deoxynucleoside triphosphate triphosphohydrolase *SAMHD1* (5), the adenosine deaminase-1 *ADARI* (6), or the cytosolic dsRNA sensor *MDA5* (7). The resulting proteins of those genes are important in nucleic acid metabolism. Mutations, in at least *TREX1*, lead to the accumulation of nucleic acids in cells, mimicking a viral infection and, in turn, activating the innate immune response (8–10).

The activation of an antiviral state in cells triggered by the accumulation of nucleic acids usually leads to increased production of IFN- $\alpha$ . Indeed, the presence of high levels of IFN- $\alpha$  in CSF and serum from AGS patients has been identified as one of the critical hallmarks of the disease (11). The levels of IFN- $\alpha$  are higher in the CSF than in the serum of patients, which indicates both extracerebral and intrathecal production (11). Our group has identified astrocytes as the major source of this IFN- $\alpha$ . These are also responsible for the increase in chemokines, such as CXCL10, in the brain of AGS patients (12). AGS patients also present elevated CSF levels of FMS-related tyrosine kinase 3 ligand, IL-12p40, IL-15, TNF- $\alpha$ , and soluble IL-2 receptor (13). Interestingly, whereas most cytokines decrease exponentially with age in the CSF of patients, CXCL10 levels are persistently elevated beyond early childhood (13). Similar observations have been described for IFN-stimulated genes (ISGs). The IFN signature in AGS patients includes genes such as *IFI27*, *IFI44L*, *IFIT1*, *ISG15*, *RSAD2*, and *SIGLEC1*. This specific ISG signature is apparently sustained over time and is currently being evaluated as a disease biomarker (14).

During the last years, different laboratories have developed knockout mouse models to study the molecular pathogenesis of AGS.

\*Department of Astrocyte Biology and Neurodegeneration, Netherlands Institute for Neuroscience, Institute of the Royal Netherlands Academy of Arts and Sciences, 1105 BA Amsterdam, the Netherlands; <sup>†</sup>Department of Experimental Immunology, Academic Medical Center, University of Amsterdam, 1105 AZ Amsterdam, the Netherlands; <sup>‡</sup>Department of Genome Analysis, Academic Medical Center, 1105 AZ Amsterdam, the Netherlands; <sup>§</sup>Department of Translational Neuroscience, Brain Center Rudolf Magnus, University Medical Center Utrecht, 3584 CG Utrecht, the Netherlands; <sup>¶</sup>Department of Pediatric Oncology, Erasmus Medical Center, 3015 CN Rotterdam, the Netherlands; <sup>||</sup>Centre National de la Recherche Scientifique, Unité Mixte de Recherche 8104, Institut Cochin, Université Paris Descartes, INSERM, Paris 75014, France; <sup>#</sup>Dipartimento di Biotecnologie e Bioscienze, Università degli Studi di Milano-Bicocca, Milan 20126, Italy; and <sup>\*\*\*</sup>Center for Neuroscience, Swammerdam Institute for Life Sciences, University of Amsterdam, 1098 XH Amsterdam, the Netherlands

<sup>1</sup>I.M. and E.J.v.B. contributed equally to this work.

Received for publication May 27, 2014. Accepted for publication February 11, 2015.

This work was supported by European Union Seventh Framework Programme Grant 241779 and by Netherlands Organization for Scientific Research Vici Grant 865.09.003 (to E.M.H.).

Address correspondence and reprint requests to Dr. Eloy Cuadrado at the current address: Department of Pediatric Hematology, Immunology and Infectious Disease, Academic Medical Center, University of Amsterdam, Meibergdreef 9, 1105 AZ Amsterdam, the Netherlands. E-mail address: eloycua@gmail.com

The online version of this article contains supplemental material.

Abbreviations used in this article: AGS, Aicardi–Goutières syndrome; CSF, cerebrospinal fluid; EdU, 5-ethynyl-2'-deoxyuridine; hCMEC, human cerebral microvascular endothelial cell; HEK, human embryonic kidney; ihNSC, immortalized human neural stem cell; ISG, IFN-stimulated gene; LV, lentiviral vector; MOI, multiplicity of infection; NT, nontargeting; shRNA, short hairpin RNA; VEGF, vascular endothelial growth factor.

Copyright © 2015 by The American Association of Immunologists, Inc. 0022-1767/15/\$25.00

*Trex1*-null mutant mice exhibit a reduced survival and develop inflammatory myocarditis, but a cerebral phenotype has never been observed (10, 15). Ablation of *Rnaseh2b* in mice leads to early embryonic lethality due to elevated DNA damage and p53-dependent growth arrest (16, 17). *Adar1*-null mutations also result in a widespread apoptosis in many tissues, as well as embryonic lethality (18). In contrast, *Samhd1*-null mutant mice do not develop any obvious pathology or autoimmunity (19, 20). All of these AGS animal models fail to replicate cerebral AGS-like symptoms and are therefore not suitable to study the intricate complexities of AGS neuropathology. Thus, human *in vitro* models are needed to study the cerebral alterations occurring in AGS (21). These models provide a unique tool to study AGS brain-related disease that otherwise would be limited to postmortem studies or imaging.

Early neuropathological human studies already suggested that AGS might represent a primary microangiopathy, because vascular mineral deposits and cortical microinfarctions were occasionally found in postmortem brains (22, 23). Recent clinical reports have described the presence of cerebrovascular disease, including ischemic and hemorrhagic strokes, in AGS patients carrying mutations for different genes (24–28). These clinical observations tie in with findings from our group describing that human astrocytes chronically exposed to IFN- $\alpha$  decrease the expression and release of proangiogenic and vascular trophic factors (21). Taken together, these observations suggest that an inflammatory disturbance of vascular homeostasis may be important in the pathogenesis of AGS.

The present study aims to gain deep insight into the specific role of each AGS gene in the biology of two important cell types of the gliovascular unit, which is part of the blood–brain barrier. To this end, short hairpin RNAs (shRNAs) against specific AGS genes were delivered to astrocytes and endothelial cells using lentiviral particles. This strategy resulted in the permanent knockdown of the targeted AGS genes, allowing us to study AGS pathogenesis in human cells, to our knowledge, for the first time in detail. We found that AGS protein knockdown leads to an increased but differential cytokine and IFN expression for both cell types tested. Interestingly, this effect was most dramatic after targeting *TREX1* in both astrocytes and endothelial cells, which fits with the observation that patients carrying mutations in *TREX1* suffer from the most severe phenotype (2) and with the observation that *Trex1*-null mutant mice have a strong IFN signature, which is weaker in *Samhd1* knockout mice (19, 20). Our approach revealed novel links between the disease severity and the production of proinflammatory mediators.

## Materials and Methods

### Cell culture

Immortalized human neural stem cells (ihNSCs), derived from neural stem cells from the diencephalic and telencephalic brain regions of one human fetus, were cultured and propagated as previously described (29). Briefly, neurospheres were cultured in Euromed-N medium (Euroclone, Pero, Italy) supplemented with 25  $\mu$ g/ml insulin, 100  $\mu$ g/ml apotransferrin, 6.3 ng/ml progesterone, 9.6 mg/ml putrescine, 520 ng/ml sodium selenite (N2 supplement, all from Sigma-Aldrich, St. Louis, MO), 20 ng/ml epidermal growth factor, and 10 ng/ml fibroblast growth factor 2 (both from Tebu-Bio, Heerhugowaard, the Netherlands) in uncoated dishes. ihNSCs were differentiated into astrocytes as described previously (21). Briefly, neurospheres were seeded at a density of 20,000 cells/ml onto laminin-coated plates and grown for 21 d *in vitro* in normal supplemented Euromed-N medium in the presence of 2% FBS without growth factors.

Human cerebral microvascular endothelial cells (hCMEC/D3) were provided by P.O. Couraud (Institut Cochin, Paris, France). Cells were grown in collagen-coated plates in EBM-2 medium supplemented with hydrocortisone, vascular endothelial growth factor (VEGF), human fibroblast growth factor, R3 insulin-like growth factor, human epidermal growth factor, GA-1000, ascorbic acid, heparin (all from Lonza, Walkersville, MD), and 2.5% FBS.

Primary human astrocytes were isolated from postmortem subcortical white matter as described previously (30). The cells were plated in wells

precoated with poly-L-lysine (Sigma-Aldrich). Cells were kept in DMEM/F12 medium containing 5% FBS, 1% penicillin/streptomycin, and 1% L-glutamine (all from Life Technologies, Bleiswijk, the Netherlands).

### shRNA constructs

shRNA expression plasmids (Supplemental Table I) from the the RNAi Consortium library (31) were obtained from Sigma-Aldrich. The plasmids express 52-bp shRNA molecules with a 21-nucleotide mRNA specificity and are driven by the ubiquitously active U6 snRNA promoter in the pLKO.1 vector backbone. Vectors containing a nontargeting (NT) sequence of the human genome (NT-shNRA, SHC002, MISSION nontarget shRNA control vector) or GFP (SHC003, MISSION TurboGFP control vector) from Sigma-Aldrich were used as controls. The efficiency of shRNA was first tested in human embryonic kidney (HEK)293T cells prior lentiviral vector (LV) production, and only the most effective shRNA vector per gene was used in the subsequent experiments in the present study.

### LV production and knockdown experiments

Recombinant LVs were produced as described previously (32) by transfecting confluent HEK293T cells with packaging (pCMV-dR8.74) and envelope plasmids (pMD2.G) with vectors (pLKO.1) containing an NT sequence, TurboGFP, or shRNAs against the genes of interest. HEK293T cells were seeded at  $12.5 \times 10^6$  cells/ml in 15-cm dishes and cultured in 20 ml DMEM (Life Technologies) supplemented with 10% FBS and 1% penicillin/streptomycin. Polyethylenimine (Roche Diagnostics, Mannheim, Germany) was used as a transfection reagent. Exactly 24 h after transfection, the cell medium was refreshed with 2% FBS and 1% penicillin/streptomycin. Finally, 24 h later, LVs were concentrated and purified by ultracentrifugation at  $50,000 \times g$  for 2.5 h at 8°C. The LVs were aliquoted and stored at  $-80^\circ\text{C}$ . Titration of harvested LVs was assessed by using a HIV-1 p24 coat protein ELISA (NEN Research Products, Boston, MA). LV titers were correlated to titers estimated by counting GFP fluorescent cells of the TurboGFP control vector.

LV stocks were used to transduce hCMEC/D3 and ihNSCs. The exact multiplicity of infection is indicated in each figure legend. Forty-eight hours postinfection, transduced cells were selected by puromycin treatment (2  $\mu$ g/ml). The knockdown efficiency was determined by both quantitative RT-PCR and Western blot.

### RNA isolation, cDNA synthesis, and quantitative real-time PCR

RNA from cell pellets was isolated as described (33) using TRIsure (Bioline, Taunton, MA) and precipitated overnight at  $-20^\circ\text{C}$  in isopropanol. Total RNA was DNase I treated and used as a template to generate cDNA following the manufacturer's instructions (QuantiTect reverse transcription kit; Qiagen, Hilden, Germany) with a blend of oligo(dT) and random hexamer primers. The reverse transcriptase reaction was incubated at  $42^\circ\text{C}$  for 30 min. The resulting cDNA was diluted 1:10 and served as a template in real-time quantitative PCR assays (SYBR Green PCR Master Mix; Applied Biosystems, Warrington, U.K.). Sequences of primers used are given in Supplemental Table II. GAPDH and  $\beta$ -actin were used as reference genes to normalize the assessed transcript levels of the target genes.

### Western blot

Protein was isolated from cells by homogenization in lysis buffer (100 mM NaCl, 10 mM Tris-HCl [pH 7.6], 1 mM EDTA [pH 8.0]) supplemented with protease inhibitors PMSF (100 mg/ml) and aprotinin (0.5 mg/ml) mixture (Roche). Protein content was determined using the BCA protein assay kit (Thermo Scientific, Rockford, IL). The same amounts of protein were dissolved in 4 $\times$  loading buffer (100 mM Tris, 4% SDS, 20% glycerol, 200 mM DTT, 0.006% bromophenol blue) that contained 5% 2-ME, and then boiled for 5 min. Subsequently, they were run on 10–15% SDS-PAGE gels and blotted semidry on nitrocellulose. Blots were blocked in SuperMix (0.606% Tris, 0.9% NaCl, 0.25% gelatin [pH 7.4]) and incubated overnight with primary Abs: rabbit anti-TREX1 (1:300, Rab34, a gift of Dr. Tomas Lindahl), rabbit anti-RNASEH2A (1:2000, Origene, Rockville, MD, TA306706), mouse anti-SAMHD1 (1:1000, Abcam, Cambridge, U.K., Ab67820), rabbit anti-ADAR1 (1:1000, Sigma-Aldrich, HPA003890), and mouse anti- $\beta$ -actin (1:4000, Developmental Studies Hybridoma Bank, Iowa City, IA, JLA20). The next day, the blots were washed with TBST (100 mM Tris-HCl [pH 7.4], 150 mM NaCl, with 0.2% Tween 20) and incubated with secondary Ab anti-rabbit IRDye 800 or anti-mouse Cy5 (1:2000, Jackson ImmunoResearch Europe, Suffolk, U.K.) in SuperMix for 1 h at room temperature. After three washes in TBST, bands were visualized with the Odyssey infrared imaging system (LI-COR Biosciences, Lincoln, NE). Cell lysates from recombinant proteins were used as positive control: TREX1 (pcDNA4.TREX1orf, gift of

R.R. Klever and A. van den Maagdenberg), RNASEH2A (Origene, LY416666), SAMHD1 (pCMV:hEF1a-SAMHD1orf), and ADAR1 (pCMV6-ADAR1orf, both gifts of J.L. van Hamme and T. Booiman).

### Cell cycle and proliferation analyses

For cell cycle analysis, cells were seeded into 24-well plates (200,000 cells/ml) and cultivated for 48 h. Cells were harvested, washed once with PBS, and fixed in 70% ice-cold ethanol for 30 min. Cells were then washed in PBS and incubated with 0.5  $\mu$ g/ml RNase T1 (Boehringer Ingelheim, Alkmaar, the Netherlands) for 15 min. Cells were washed again and incubated with 2.5  $\mu$ g/ml propidium iodide (Sigma-Aldrich). Cells were analyzed on a BD FACSCanto II flow cytometer (BD Biosciences, San Jose, CA).

Cell proliferation was measured using the Click-iT 5-ethynyl-2'-deoxyuridine (EdU) flow cytometry assay kit (Life Technologies Europe) according to the manufacturer's instructions. Using the standard protocol, the cells were incubated with 2.5  $\mu$ M EdU for 2 h at 37°C. After that period the cells were fixed and permeabilized, and EdU was detected by adding the Click-iT reaction mixture in the dark. After 30 min, cells were washed and FACS analysis was immediately performed using the BD FACSCanto II flow cytometer (BD Biosciences). Collected data were analyzed using FlowJo software version 7.6.3 (Tree Star, Palo Alto, CA).

### Immunocytochemistry

Immunostaining was performed according to a standard protocol. Briefly, cells were fixed in 4% ice-cold paraformaldehyde for 15 min. The wells were then washed with PBS and permeabilized for 10 min with PBS containing 0.25% Triton X-100. Subsequently, cells were washed again with PBS and blocked for 30 min in SuperMix. After blocking, cells were incubated overnight at 4°C with the following primary Abs: mouse anti-GFAP (1:1000, Sigma-Aldrich, G3893), rabbit anti-S100B (1:600, Dako, Glostrup, Denmark, Z0311), rabbit anti-cleaved caspase-3 (1:400, Cell Signaling Technology, Danver, MA, 9661), mouse anti-CD31 (1:100, Dako), and chicken anti-vimentin (1:1000, Millipore, Billerica, MA, AB5733). The following day, cells were washed three times in PBS and incubated with Cy3- or Cy2-labeled secondary Abs (1:500, Jackson ImmunoResearch Laboratories, Newmarket, Suffolk, U.K.) diluted in SuperMix for 1 h at room temperature in the dark. Finally, cells were washed three more times in PBS and nuclei were counterstained with 1  $\mu$ g/ml Hoechst. Stainings were analyzed with a fluorescence microscope (Zeiss 200M Axiovert, Carl Zeiss, Sliedrecht, the Netherlands) interfaced with an image analysis system (Image-Pro Plus 6.3, Media Cybernetics, Bethesda, MD).

### Cell migration scratch assay

The scratch assay was carried out as described before by others (34). Briefly,  $1 \times 10^6$  cells were seeded in 24-well plates. The following morning, a 20- $\mu$ l plastic pipette tip was used to draw across the wells to create a linear region void of cells. Afterward, wells were washed and medium was refreshed. Initial images of the denuded zone were taken immediately ( $t = 0$  h) using an inverted microscope (Zeiss 200M Axiovert, Carl Zeiss). Plates were then incubated at 37°C and images were taken after 24 and 48 h. Images of the same fields were captured and analyzed using imaging software (ImageJ, version 1.43u, National Institutes of Health, Bethesda, MD).

### Tubulogenesis/Matrigel

For the Matrigel assay, hCMEC/D3 cells were seeded onto 96-well plates coated with growth factor-reduced Matrigel (BD Biosciences) at a density of 100,000 cells/well. After 16 h, digitized images of four representative fields were taken (at  $\times 5$  magnification) in bright field using the Zeiss 200M Axiovert microscope. The number of complete rings and the total tube length were measured using the ImageJ software as described by others (35).

### Luminex

Briefly, 25- $\mu$ l supernatants were analyzed using a custom Bio-Plex Pro human cytokine 27-plex panel Ab kit according to the manufacturer's protocol (Bio-Rad, Veenendaal, the Netherlands). Plates were read on a BioPlex protein array system (Bio-Rad) using the standard high and low calibration curves. Data analysis was performed using Bio-Plex Manager software (Bio-Rad).

### Statistical analysis

All experiments were performed at least three independent times unless otherwise specified. Graphs are presented as bar charts with  $\pm$  SEM. The IFN score was calculated from the median fold change value for a panel of seven IFN-stimulated genes (*IFIT1*, *IFIT2*, *IFIT3*, *IRF9*, *OAS1*, *IFI27*, and *RSAD2*) as described previously (14). The variable distribution was assessed by the Kolmogorov-Smirnov test. When the test distribution was not normal,

a nonparametric Kruskal-Wallis test was used followed by a Dunn's multiple comparison test to assess intergroup differences. Luminex data were analyzed using the nonparametric Friedman test for paired groups followed by a Dunn multiple comparison test to assess intergroup differences. A  $p$  value  $< 0.05$  was considered statistically significant at a 95% confidence level. Tests were performed as indicated using Prism 6.0 (GraphPad Software, San Diego, CA).

## Results

### Inhibition of *TREX1* by *shRNA* induces apoptosis in human astrocytes

To study the significance of AGS genes in the astrocyte homeostasis, ihNSCs were differentiated into astrocytes (Fig. 1A) and subsequently transduced with LVs expressing shRNAs targeting the different AGS genes. Afterward, the protein expression of *TREX1*, *SAMHD1*, *RNASEH2A*, and *ADAR1* was examined and found to be reduced as compared with NT shRNA-transduced cells (Fig. 1B). Previously published data showed that deletion or knockdown of one of the three subunits of the RNASEH2 protein complex is sufficient for the elimination of its activity (16). Although we could not detect *SAMHD1* protein in our astrocyte lysates, we were able to detect *SAMHD1* mRNA. These findings are in accordance with the gene atlas analysis showing a minimal expression of *SAMHD1* in neural tissues (36). Moreover, we observed a major decrease in *SAMHD1* mRNA upon knockdown (Supplemental Fig. 1).

An early observation suggested that silencing *TREX1* in astrocytes resulted in a decreased cell survival. Indeed, the higher the multiplicity of infection (MOI) we used, the lower was the number of surviving cells (Fig. 1C). The effect was already evident with a low MOI, excluding a general toxic effect of the *TREX1* shRNA. At higher MOIs, the number of *TREX1* shRNA-transduced cells was decreased up to 70% compared with the NT shRNA control ( $p < 0.01$ , Fig. 1C, 1D). This effect on survival was not paralleled in the other control or AGS gene shRNA-transduced cell cultures. Only *ADAR1* shRNA-transduced cells presented a slight, non-significant reduction. Because many floating cells were found in *TREX1*-transduced cultures, the cells were also stained against cleaved caspase-3. Indeed, we found a high number of positive cells (Fig. 1E) and conclude that *TREX1* silencing reduces the number of surviving astrocytes by inducing apoptosis.

### Silencing of *TREX1* results in a reduced proliferation of endothelial cells

To assess the importance of AGS genes in human brain-derived microvascular endothelial cells, hCMEC/D3 cells were transduced with LVs expressing shRNAs targeting the different AGS genes (Fig. 2A). The expression of *TREX1*, *SAMHD1*, *RNASEH2A*, and *ADAR1* was significantly reduced in the knockdown cells compared with NT shRNA-transduced cells at mRNA (Supplemental Fig. 2) and protein levels (Fig. 2B).

Next, we studied the effect of silencing AGS genes on the proliferation of hCMEC/D3 cells. Transduction with the different LVs had no visible effect on the cells, and cell death was not observed. However, we did notice a reduced proliferation of *TREX1* shRNA-transduced cells. To further investigate this, we used EdU to pulse label cells for 2 h, allowing EdU to incorporate into all dividing cells. We then quantified the amount of EdU integration by flow cytometry (Fig. 2C). This method enumerates the proportion of cells progressing through the cell cycle during the short pulse labeling and therefore overcomes confounders such as cell death (37). We found that the proportion of EdU<sup>+</sup> cells was significantly reduced in *TREX1* shRNA-transduced cells ( $p < 0.05$ , Fig. 2D). Moreover, to evaluate a possible cell cycle defect in knockdown cells, we determined the proportion of cells in each phase of the cycle in asynchronous endothelial cell cultures (Fig. 2E). However,

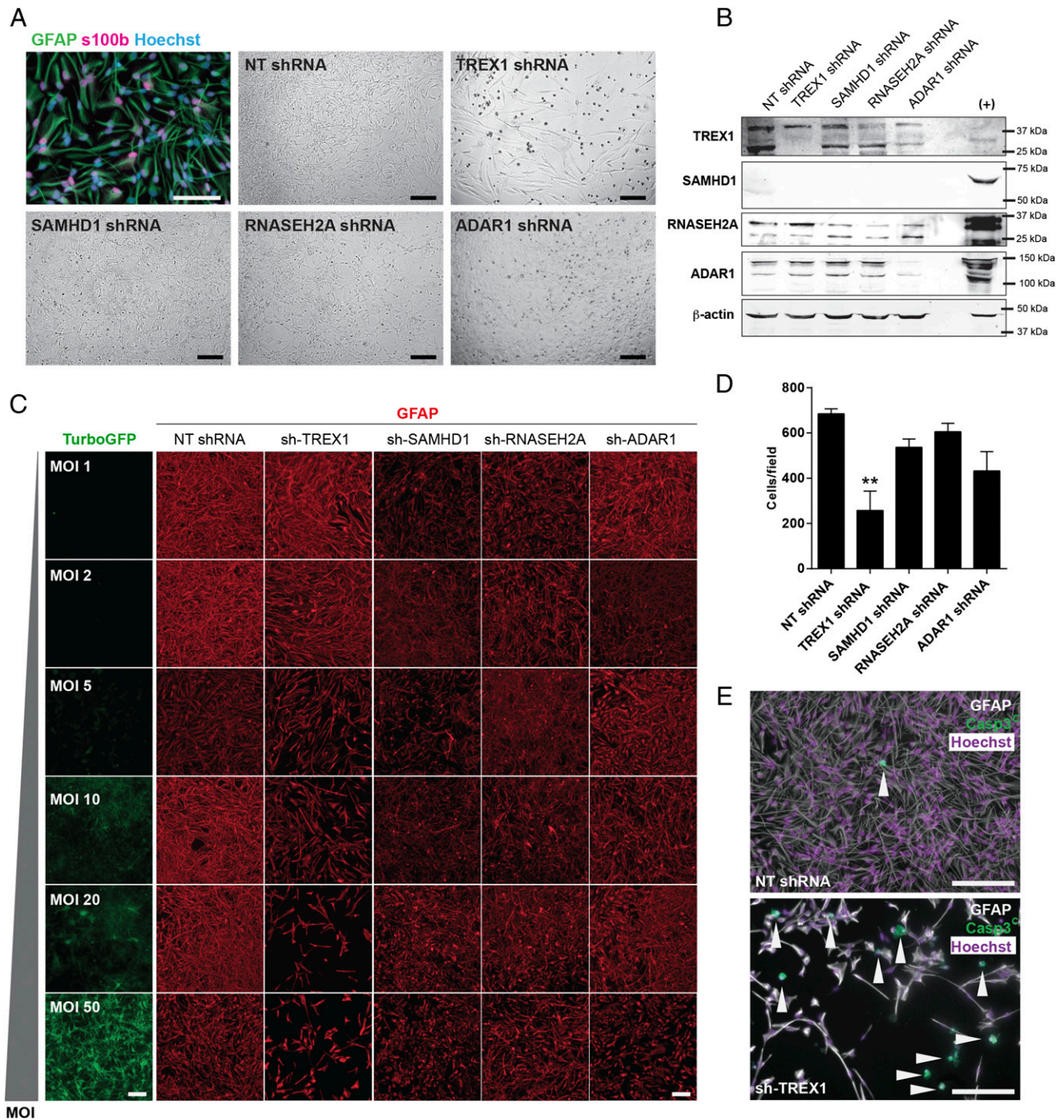


**FIGURE 1.** Effect of knockdown on iNSC-derived astrocytes. **(A)** Immunostaining of cells against the astrocytic markers GFAP (in green) and S100B (in magenta). Nuclei are counterstained with Hoechst (in blue). Phase-contrast images are from cells transduced with AGS shRNAs. **(B)** Representative immunoblots from cell lysates confirm the knockdown of *TREX1*, *SAMHD1*, *RNASEH2A*, and *ADAR1*, respectively. Cell lysates from cells overexpressing the respective recombinant human protein were loaded as a positive control (+). Actin was detected as loading control. **(C)** First column of images corresponds to endogenous fluorescence of cells expressing GFP (in green) after transduction with the positive control SHC003-TurboGFP. Panels show immunostainings of transduced astrocytes against GFAP (in red) with increasing MOI (range, 1–50). **(D)** Graph shows quantification of number of cells per field after transduction with the different shRNAs ( $n = 3$ ). Data represent means  $\pm$  SEM.  $**p < 0.01$ . **(E)** Immunostaining of NT- and *TREX1* shRNA-transduced cells against GFAP (in white) and cleaved caspase-3 (in green). Nuclei are counterstained with Hoechst (in purple). Caspase-3<sup>+</sup> cells are indicated by arrowheads. Scale bars, 100  $\mu$ m.

quantitative FACS analysis revealed only a minor reduction in the proportion of *TREX1* shRNA-transduced cells in  $M/G_2$  phase compared with control cells (Fig. 2F).

#### AGS genes are not essential for in vitro vasculogenesis

Endothelial cell migration and tube formation in Matrigel are widely used as in vitro assays for angiogenesis (38). To show the involve-

ment of AGS gene silencing in capillary morphogenesis, endothelial knockdown cells were seeded on a Matrigel matrix (Fig. 3A). We analyzed the tube formation by measuring the length of the tubules (Fig. 3B) and the number of rings (Fig. 3C) formed by the cells on the matrix. We observed no differences in the knockdown cells compared with controls, demonstrating that silencing AGS genes does not affect the tubulogenic capacity of endothelial cells in vitro.

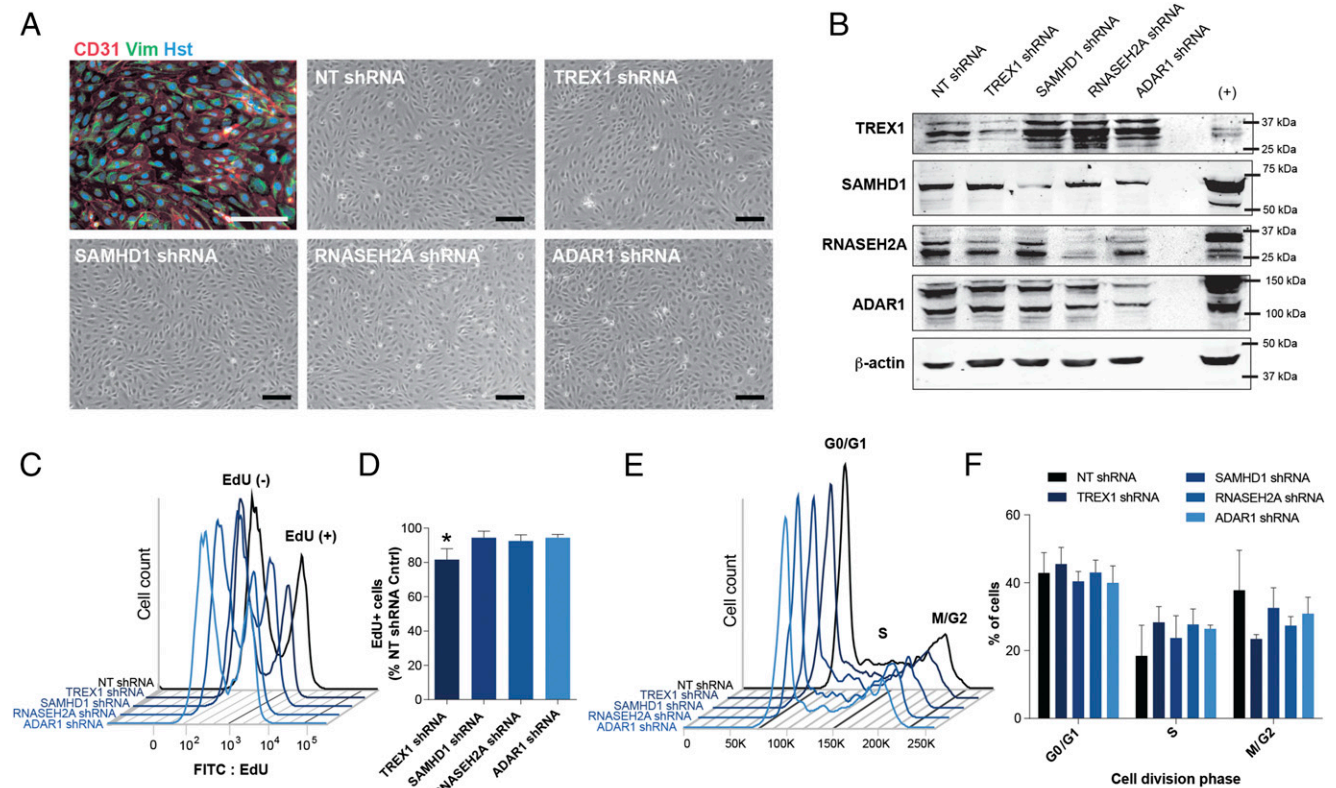


**FIGURE 2.** Effect of knockdown on hCMEC/D3 cells. **(A)** Immunostaining of cells against the endothelial markers CD31 (in red) and vimentin (in green). Nuclei are counterstained with Hoechst (in blue). Phase-contrast images are from cells transduced with AGS shRNAs. Scale bars, 100  $\mu$ m. **(B)** Representative immunoblots from cell lysates confirming the knockdown of *TREX1*, *SAMHD1*, *RNASEH2A*, and *ADAR1*, respectively. Lysates from cells overexpressing the respective recombinant human protein were loaded as a positive control (+). Actin was used as loading control. **(C)** Histogram showing the number of cells that are Edu-FITC negative (–) and positive (+) in the different transduced cells. **(D)** Bar graph showing the quantification of Edu<sup>+</sup> cells compared with NT control in percentage ( $n = 5$ ). Data represent means  $\pm$  SEM. \* $p < 0.05$ . **(E)** Histogram showing the cell cycle distribution of asynchronous cultures. **(F)** Bar graph showing the quantification of cells in G<sub>0</sub>/G<sub>1</sub>, S, and G<sub>2</sub>/M phases ( $n = 4$ ). Data represent means  $\pm$  SEM.

Interestingly, shRNA silencing of *TREX1* in endothelial cells resulted in a reduced migration of those cells compared with control cells (Fig. 3D, 3E) after 24 ( $p < 0.05$ ) and 48 h ( $p < 0.001$ ). *TREX1* shRNA-transduced cells also showed a reduced migration capacity compared with other shRNA-treated cells after 48 h ( $p < 0.001$ ).

#### Silencing AGS genes activates the expression of ISGs

Increasing evidence exists that IFN- $\alpha$  is not only a potent biomarker in AGS, but also a key player in AGS pathogenesis. We therefore studied the production of IFN- $\alpha$  and the ISGs in astrocytes and endothelial cells after silencing AGS genes.

IFN- $\alpha$  expression was induced in astrocytes after silencing of *TREX1* ( $p < 0.05$ , Fig. 4A) but not after knocking down the expression of the other AGS genes. Likewise, the expression of MHC I (*HLA-C*), which is known to be induced by IFN- $\alpha$ , was increased only in *TREX1* knockdown cells ( $p < 0.05$ , Fig. 4B). In contrast, endothelial cells showed no induction of either IFN- $\alpha$  or *HLA-C* upon silencing of any AGS gene (Fig. 4C, 4D).

When the expression of a panel of ISGs was studied, we observed increased *OAS1* expression in astrocytes after silencing *TREX1*, *SAMHD1*, or *ADAR1*, but not after silencing *RNASEH2A* (Fig. 4E). Also, the overall IFN score was not increased in astrocytes compared with control shRNA-transduced cultures (Fig. 4F). The IFN score was calculated with the median fold changes of seven ISGs, as indicated in *Materials and Methods*, and represents the responsiveness to IFN. In contrast, we observed a significant increase in the mRNA expression of *IFIT1* ( $p < 0.05$ ), *IFIT2* ( $p < 0.05$ ), *IFIT3* ( $p < 0.05$ ), *IRF9* ( $p < 0.01$ ), *OAS1* ( $p < 0.05$ ), *IFI27* ( $p < 0.05$ ),

and *RSAD2* ( $p < 0.05$ ) in *TREX1* knockdown endothelial cells (Fig. 4G). *SAMHD1* knockdown endothelial cells also showed an increased expression of transcripts for *IFIT2* ( $p < 0.01$ ), *IFIT3* ( $p < 0.05$ ), and *IRF9* ( $p < 0.05$ ). No effects, however, were seen in the case of *ADAR1* or *RNASEH2A* silencing on endothelial cells. The overall IFN score for *TREX1*-depleted cells was higher than that for NT shRNA control cells (Fig. 4H).

#### Silencing of *TREX1* results in an increased production of proinflammatory and chemotactic cytokines

In addition to IFN- $\alpha$ , the chemokine CXCL10 has also been described to be elevated in CSF and plasma from AGS patients. *CXCL10* expression is highly induced in astrocytes after silencing of *TREX1* ( $p < 0.01$ ), *SAMHD1* ( $p < 0.001$ ), and *ADAR1* ( $p < 0.05$ ; Fig. 5A). However, the induction of *CXCL10* after silencing of *RNASEH2A* was much weaker compared with all other genotypes. Noticeably, only the ablation of *TREX1* resulted in a clear induction of *CXCL10* expression in endothelial cells ( $p < 0.05$ ; Fig. 5B).

We also measured the cytokines and chemokines released by astrocytic and endothelial cell cultures after 21 and 7 d, respectively. In astrocytes, silencing of *TREX1* resulted in a moderate release of the cytokine IL-6 ( $p < 0.05$ ), as well as a substantial release in the chemokines CXCL10 ( $p < 0.05$ ) and CCL5 ( $p < 0.05$ ; Fig. 5C). These results are similar to those found in endothelial cells (Fig. 5D). Silencing of *SAMHD1* only produced an increased release of CXCL10 ( $p < 0.01$ ) and CCL5 ( $p < 0.01$ ) in astrocyte cultures but not in endothelial cells. Silencing of *ADAR1* or *RNASEH2A* did not induce any obvious increase in the production of cytokines in these cultures.

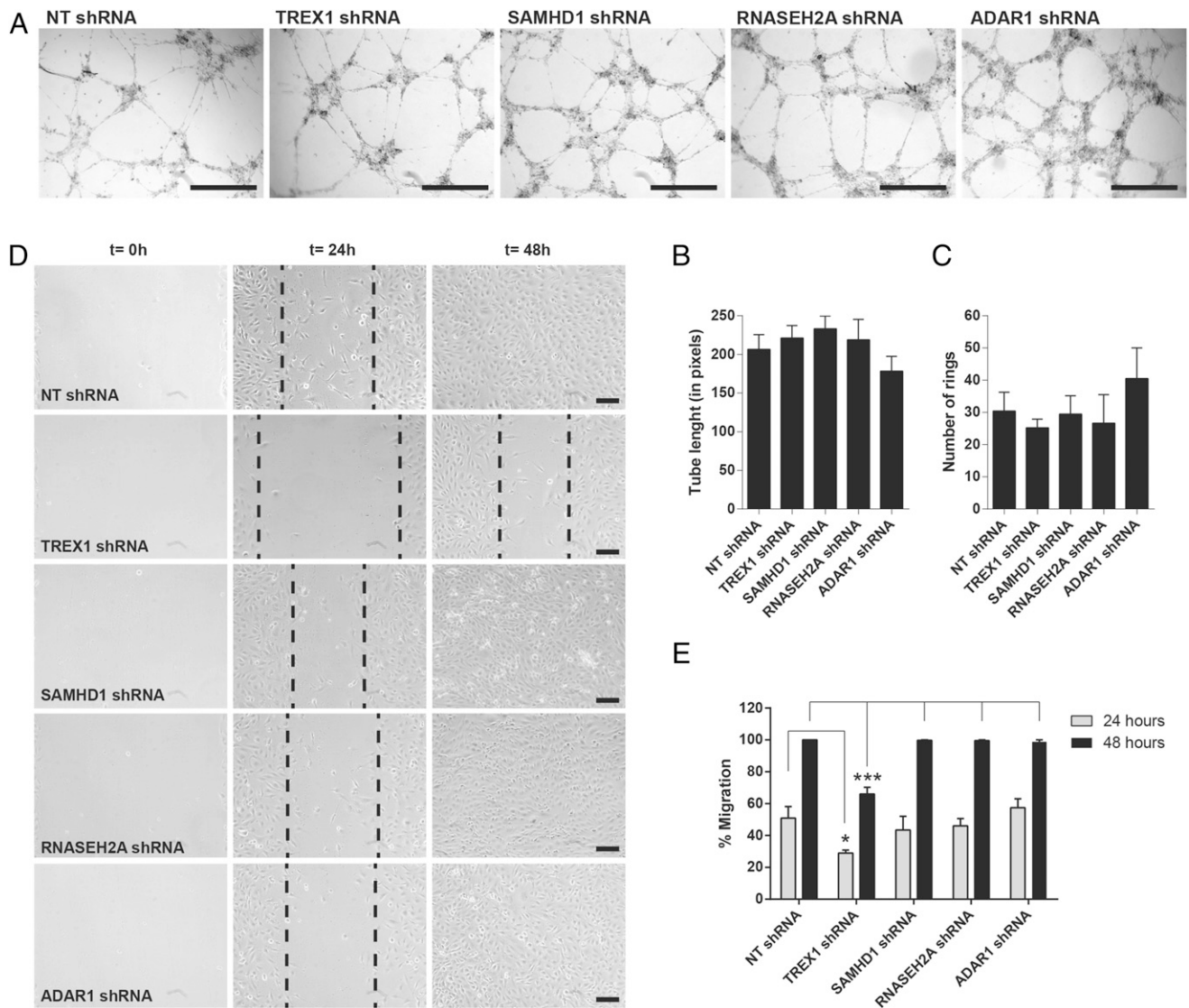


**FIGURE 3.** AGS gene silencing effect on vasculogenesis and migration in hCMEC/D3 cells. **(A)** Representative phase-contrast images of tube formation assay on Matrigel. Scale bars, 500  $\mu\text{m}$ . Bar graphs showing the quantification of the total length (in pixels) **(B)** and the mean number of rings **(C)** ( $n = 4$ ). Data represent means  $\pm$  SEM. **(D)** AGS gene shRNA-transduced cells were subjected to scratch migration assay. The plates were photographed at the identical location of the initial image at  $t = 24$  h and  $t = 48$  h after the generation of the scratch. Dashed line notes the approximate edge of the wound. Scale bars, 100  $\mu\text{m}$ . **(E)** Graph showing the percentage of cell migration after 24 (gray bars) and 48 h (blue bars) ( $n = 3$ ). Data represent means  $\pm$  SEM. \* $p < 0.05$ , \*\* $p < 0.001$ .

#### Silencing of *TREX1* impairs the growth of primary human astrocytes in vitro and activates the expression of ISGs

To confirm the significance of AGS genes in the astrocyte homeostasis, the different AGS genes were knocked down in human primary astrocytes (Fig. 6A). The expression of *TREX1*, *SAMHD1*, *RNASEH2A*, and *ADAR1* was examined and found to be reduced as compared with NT shRNA-transduced cells (Fig. 6B). As observed previously in the ihNSC-derived astrocytes, the final number of *TREX1* shRNA-transduced human primary astrocytes cells was severely decreased compared with the NT shRNA control ( $p < 0.05$ , Fig. 6C).

Additionally, we measured the expression of IFN- $\alpha$  and other ISGs. IFN- $\alpha$  expression was induced in primary astrocytes only after silencing of *TREX1* ( $p < 0.05$ , Fig. 6D). When we studied the expression of a panel of ISGs, we only observed increased *IFIT2* expression after silencing *SAMHD1* ( $p < 0.05$ , Fig. 6E).

#### Discussion

An important and fundamental aspect that remains to be clarified in AGS pathogenesis is the relationship between innate immune re-

sponse, vasculopathy, and demyelination. It is unknown why a genetically heterogeneous disorder with mutations in at least six different, ubiquitously expressed genes leads to a syndrome with similar clinical manifestations and tropism for the CNS. Although the clinical picture of AGS patients may be alike in some features, these different mutations produce a diverse spectrum of phenotypes, in particular disease progression, with certain genotype/phenotype correlations. Patients carrying *TREX1* mutations present a more severe clinical picture (presenting with abnormal neurology already in the neonatal period) and higher mortality rate compared with patients carrying an *RNASEH2B* mutation (2). In another study, researchers described a distinctive CSF lymphocytes gene expression signature in AGS patients bearing different gene mutations (39), and again in the present study, patients with mutations in *TREX1* had the most severe and the earliest symptom onset. Furthermore, it has been shown that patients with *SAMHD1* mutations have a later disease onset and a generally milder phenotype (24–26).

Our study clearly shows that silencing *TREX1* resulted in a reduced viability of both ihNSC-derived astrocytes and primary

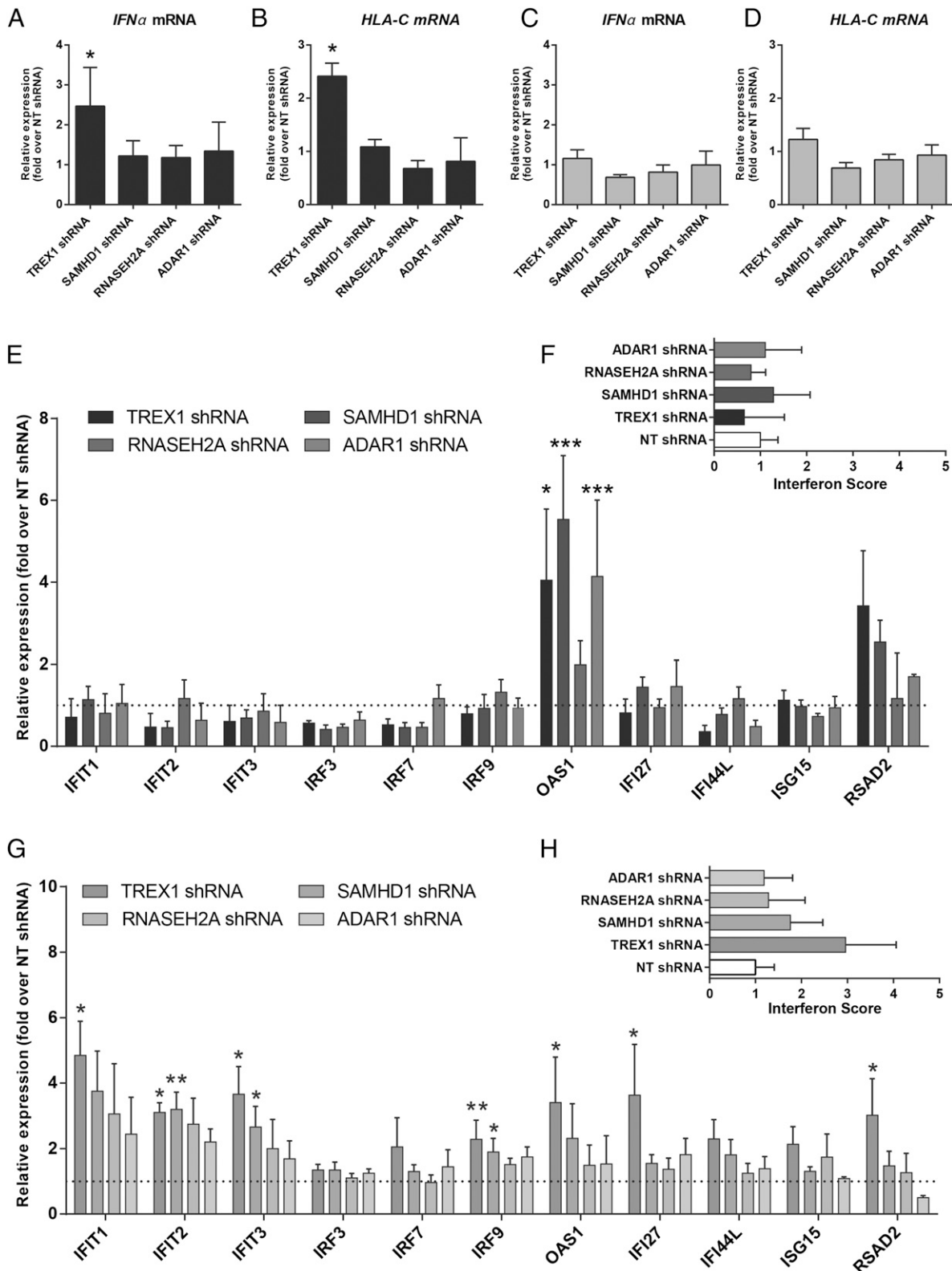


**FIGURE 4.** ISG signature activation on transduced cells. Bar graphs show *IFN-α* (**A** and **C**) and *HLA-C* (**B** and **D**) transcript levels in AGS gene shRNA-transduced astrocytes ( $n = 7$ , in black) and endothelial cells ( $n = 5$ , in gray). Normalized values are presented as fold over NT shRNA controls. (**E**) Quantitative PCR analysis of ISG mRNA expression in transduced astrocytes. Results are presented as fold over control (dashed line) and represent means  $\pm$  SEM ( $n = 7$ ). (**F**) IFN score was calculated from the median fold change from six ISGs. (**G**) Quantitative PCR analysis of ISG mRNA expression in transduced endothelial cells. Results are presented as fold over control (dashed line) and represent means  $\pm$  SEM ( $n = 5$ ). (**H**) *TREX1* knockdown cells show an increased IFN score. \* $p < 0.05$ , \*\* $p < 0.01$ , \*\*\* $p < 0.001$ .

human astrocytes, as well as a reduced proliferation of endothelial cells. Silencing of any of the other AGS-causative genes did not parallel the strong *TREX1*-related effects. The most severe effect

was observed after silencing *TREX1* in astrocytes and, to our knowledge, this is the first time that *TREX1* deficiency has been linked to cell death. Previous data on silencing *TREX1* in murine

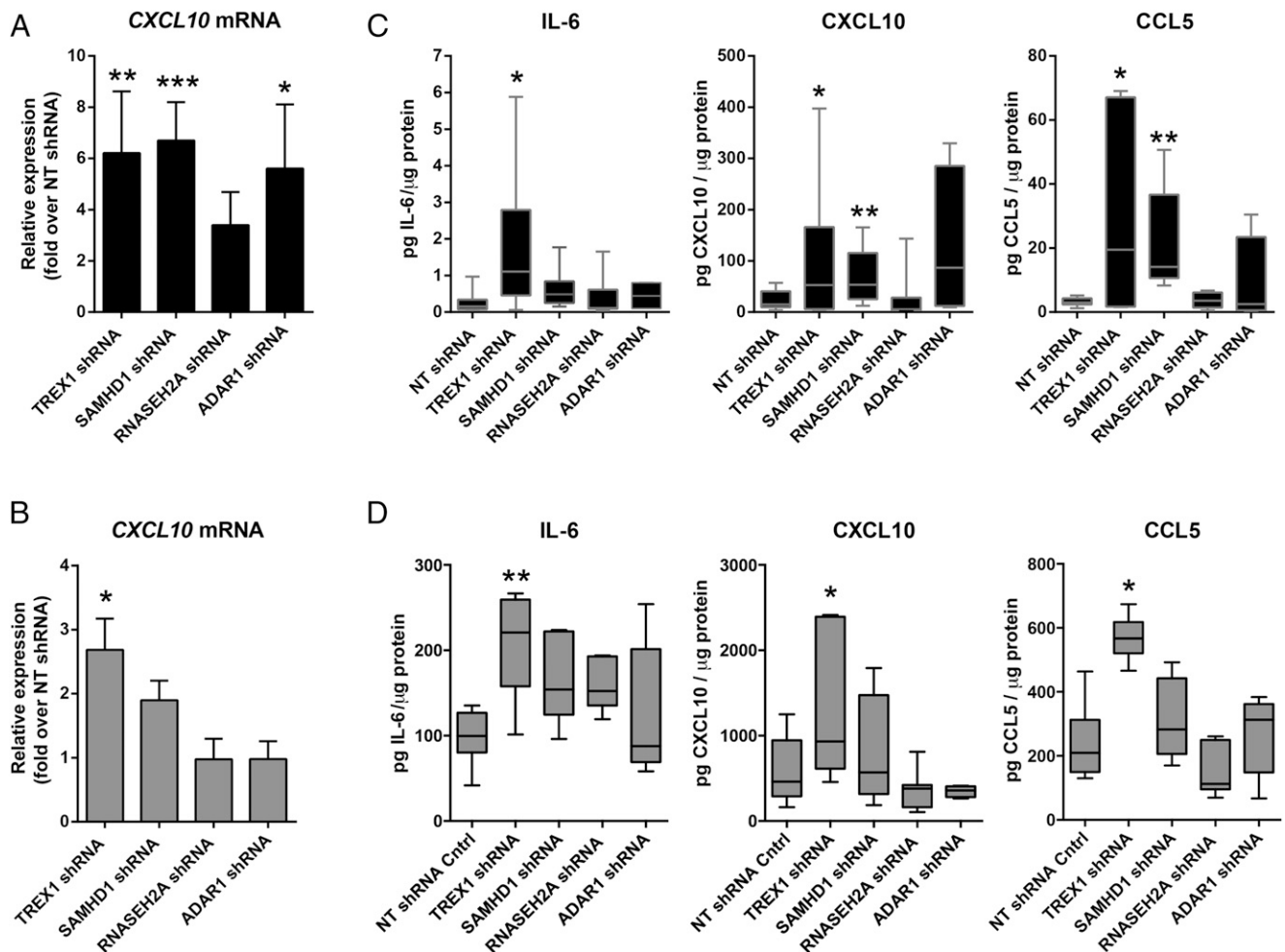


**FIGURE 5.** AGS gene knockdown induces the production and release of cytokines. Quantitative PCR analysis of *CXCL10* mRNA expression in AGS gene shRNA-transduced astrocytes (**A**) ( $n = 7$ , in black) and endothelial cells ( $n = 5$ , in gray) (**B**). Normalized values are presented as fold over NT shRNA controls. (**C**) Secreted cytokines levels were measured in the supernatant from transduced astrocytes. Results are expressed in picograms per microgram total protein (mean  $\pm$  SEM,  $n = 9$ ). (**D**) Cytokine and chemokine levels were measured in the supernatant from transduced endothelial cells. Results are expressed in picograms per microgram total protein (mean  $\pm$  SEM,  $n = 7$ ). \* $p < 0.05$ , \*\* $p < 0.01$ , \*\*\* $p < 0.001$ .

and human fibroblasts reported an impaired  $G_1/S$  cell cycle transition provoking a cell cycle arrest but not apoptosis (8). Increased apoptosis has never been reported in vivo in *Trex1*-null mutant mice (9) or in their cells cultured ex vivo (10, 40). It is also intriguing why we observe this effect so dramatically in human astrocytes and not in endothelial cells. We do describe a reduced proliferation in human *TREX1* shRNA-transduced endothelial cells. This is in line with a previous study reporting that *TREX1*-null mutant fibroblasts showed a chronic DNA damage checkpoint activation and a cell cycle arrest (8). Importantly, note that endothelial cells showed a reduced proliferation even though they are immortalized.

Other investigations have shown that also other AGS gene defects can affect proliferation. *SAMHD1*-null mutant fibroblasts have been shown to exhibit a cell cycle arrest (41). Another investigation also revealed a delayed cell cycle progression after transient knockdown of *SAMHD1* in HeLa cells using small interfering RNA (42). Alternatively, transient knockdown of *ADAR1* in HeLa cells did not alter the cell growth (43). Hence, the effect of AGS gene deficiency seems to be both tissue and cell specific.

During the last few years, it has become clear that vasculopathy is an essential feature of AGS pathophysiology. From our results, we can conclude that AGS gene mutations have only a limited effect on the normal angiogenic, vasculogenic, and proliferative capacity of

cerebral endothelial cells. This means that the vascular alterations observed previously by our group (21) and others (22) are most likely not intrinsically caused by the effect of the mutations in endothelial cells, but rather are caused by the environment. There are abundant data supporting this idea. First, AGS patients present substantial high levels of circulating IFN- $\alpha$  (11). IFN- $\alpha$  is a well-known potent antiangiogenic factor and is therefore used as coadjuvant therapy in different types of cancer (44). Second, the levels of IFN- $\alpha$  remain sustainably high for years in both serum and CSF (12, 45). Third, a general downregulation of angiogenesis-related genes has been described for AGS patients carrying different genotypes (46). Fourth, we have previously shown that IFN- $\alpha$  inhibits the production proangiogenic factors such as VEGF and IL-1 by astrocytes (21), the only VEGF-producing cells in the adult brain (47). Finally, we confirmed the downregulation of VEGF and IL-1 in AGS brain specimens (21). Taken together, these data suggest that the sustained alteration of the pool of pro- and antiangiogenic factors may lead to an abnormal vessel formation and proliferation profile in the brain of AGS patients.

Our data also show an induction of IFN- $\alpha$  specifically in *TREX1*-null mutant astrocytes and not in any other shRNA-treated cells. In fact, endothelial cells did not produce IFN- $\alpha$  after transduction with any of the shRNA particles. In endothelial cells, the expression of many ISGs is induced independently of IFN- $\alpha$ . Many ISGs

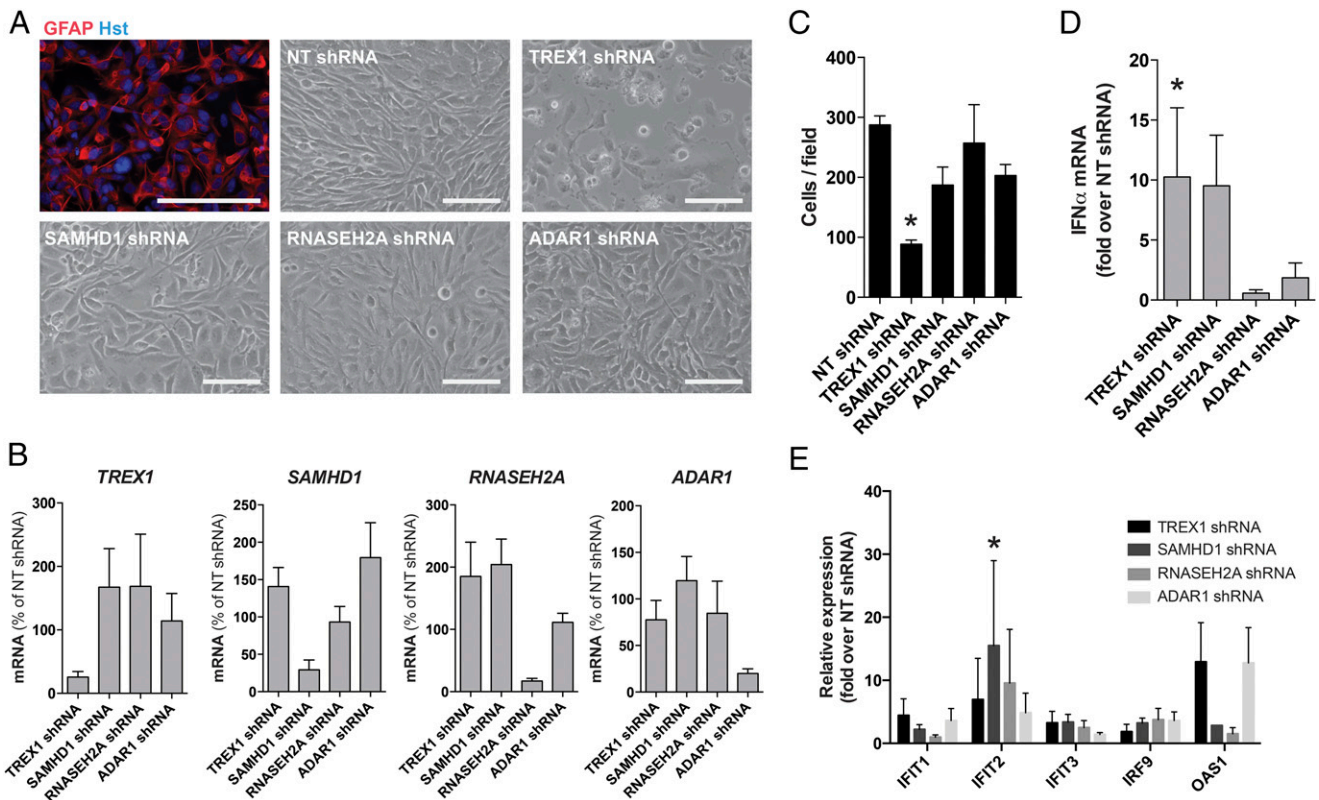


**FIGURE 6.** Effect of knockdown on human primary astrocytes. **(A)** Immunostaining of cells against the astrocytic marker GFAP (in red). Nuclei are counterstained with Hoechst (in blue). Phase-contrast images are from cells transduced with different shRNAs. Scale bars, 100 μm. **(B)** Bar graphs show AGS genes transcript levels in shRNA transduced astrocytes ( $n = 3$ ). Normalized values are presented as percentage to NT shRNA controls. **(C)** Graph shows quantification of number of cells per field after transduction with the different shRNAs ( $n = 3$ ). Data represent means ± SEM. **(D)** Quantitative PCR analysis of *IFN-α* mRNA expression in AGS gene shRNA-transduced astrocytes. **(E)** Quantitative PCR analysis of ISG mRNA expression in transduced astrocytes. Results are presented as fold over control and represent mean ± SEM ( $n = 3$ ). \* $p < 0.05$ .

(e.g., *IFIT1*) can be easily activated by IRF proteins independently of *IFN-α* (48), and independent activation of ISGs has also been demonstrated most recently in *Trex1*-null mutant and *Trex1* knockdown mouse embryonic fibroblasts (49). Our data clearly demonstrate that the knockdown of AGS genes differentially affects distinct cell types. Our findings support the unexplained findings in AGS patients, where the induction of ISGs such as *IFIT1*, *IFIT2*, *IFIT3*, *IRF3*, and *RSAD2* was detected in *TREX1*-mutated fibroblasts and not in *SAMHD1*- and *RNASEH2C*-mutated cells (49). In contrast, the same measurement in whole blood cells from AGS patients showed many ISGs independent of the genotype (14). In this latter study, only a few patients carrying mutations in *RNASEH2B* gene appeared negative for the IFN response signature. Our data confirm the minor induction of ISGs in astrocytes and endothelial cells after silencing *RNASEH2A*. However, it remains unexplained why the ISG-activation signature is stronger in *TREX1*-null mutant cells in comparison with the other genotypes.

Even though *IFN-α* is considered to be a key biomarker for AGS, the chemokine *CXCL10* has also been persistently demonstrated to have an elevated expression in AGS patients (12, 13). Consistent with this, our study shows that silencing AGS genes results in an increased expression and release of *CXCL10* mainly in astrocytes. Furthermore, our work has also provided insight into the differential profile of cytokines in the different AGS genotypes. Also in the present study, *TREX1*-null mutant cells were producing the highest levels of cytokines. Collectively, the cytokine profiles seamlessly paralleled the ISG expression. Our data have shed some light on the functional implications of an ISG activation in the context of AGS. *TREX1*-null mutant cells

present a more robust induction of ISGs that is translated into a higher expression and release of inflammatory cytokines and chemoattractants.

It has been suggested before that an IFN genetic signature may correlate with the phenotypic observations and clinical status in patients (14). We propose a model that links the chronic activation of ISGs with the cerebral autoimmune presentations observed in AGS, in which cytokines play a central role. First, patients carrying AGS gene mutations present an induction of ISGs and a sustained secretion of cytokines and chemokines. This continuous response stimulates the activation of the vasculature and facilitates the transmigration of inflammatory cells into the cerebral parenchyma. The persistent activation of the inflammatory cells might initiate demyelination. Additionally, the inflammatory disturbance of the brain vasculature may lead to prothrombotic phenomena and hypoperfusion that can contribute to demyelination. The disease severity may be reflected by higher ISG induction and cytokine secretion, with the worst prognosis in patients with a *TREX1* mutation (2, 14). Future studies to confirm this hypothesis are needed.

In summary, we describe the effect of silencing AGS genes in astrocytes and endothelial cells, two major cell types forming the gliovascular junction. Knockdown of AGS genes, especially *TREX1*, results in an activation of ISG signaling as well as a substantial release of both proinflammatory cytokines and chemokines. Our findings provide insight into how cell-differential activation of the antiviral status leads to cerebral autoimmune pathology in AGS, and they suggest a link between proinflammatory mediators and disease severity.

## Acknowledgments

We thank Dr. Tomas Lindahl (Clare Hall Laboratories, Cancer Research UK London Research Institute) for providing the anti-TREX1 Ab. We also thank John L. van Hamme and Thijs Booiman (Experimental Immunology, Academic Medical Center) for providing the plasmids used as positive controls for SAMHD1 and ADAR1 Western blots. We are also grateful to Roselin R. Klever and Dr. Arn van den Maagdenberg (Department of Human Genetics, Leiden University Medical Center, Leiden, the Netherlands) for providing the plasmid used as positive control for TREX1 Western blots. We also thank L. Naldini (Institute for Cancer Research, University of Turin Medical School, Turin, Italy) for providing the lentiviral plasmids. We thank Dr. Carlyn Martina-Mamber for valuable help in editing the manuscript. The authors acknowledge the Netherlands Brain Bank and Dr. M. van Strien for providing the brain donor material for the isolation of primary human astrocytes.

## Disclosures

The authors have no financial conflicts of interest.

## References

- Aicardi, J., and F. Goutières. 1984. A progressive familial encephalopathy in infancy with calcifications of the basal ganglia and chronic cerebrospinal fluid lymphocytosis. *Ann. Neurol.* 15: 49–54.
- Rice, G., T. Patrick, R. Parmar, C. F. Taylor, A. Aeby, J. Aicardi, R. Artuch, S. A. Montalto, C. A. Bacino, B. Barroso, et al. 2007. Clinical and molecular phenotype of Aicardi-Goutières syndrome. *Am. J. Hum. Genet.* 81: 713–725.
- Crow, Y. J., B. E. Hayward, R. Parmar, P. Robins, A. Leitch, M. Ali, D. N. Black, H. van Bokhoven, H. G. Brunner, B. C. Hamel, et al. 2006. Mutations in the gene encoding the 3'-5' DNA exonuclease TREX1 cause Aicardi-Goutières syndrome at the AGS1 locus. *Nat. Genet.* 38: 917–920.
- Crow, Y. J., A. Leitch, B. E. Hayward, A. Garner, R. Parmar, E. Griffith, M. Ali, C. Sempke, J. Aicardi, R. Babul-Hirji, et al. 2006. Mutations in genes encoding ribonuclease H2 subunits cause Aicardi-Goutières syndrome and mimic congenital viral brain infection. *Nat. Genet.* 38: 910–916.
- Rice, G. I., J. Bond, A. Asipu, R. L. Brunette, I. W. Manfield, I. M. Carr, J. C. Fuller, R. M. Jackson, T. Lamb, T. A. Briggs, et al. 2009. Mutations involved in Aicardi-Goutières syndrome implicate SAMHD1 as regulator of the innate immune response. *Nat. Genet.* 41: 829–832.
- Rice, G. I., P. R. Kasher, G. M. A. Forte, N. M. Mannion, S. M. Greenwood, M. Szykiewicz, J. E. Dickerson, S. S. Bhaskar, M. Zampini, T. A. Briggs, et al. 2012. Mutations in ADAR1 cause Aicardi-Goutières syndrome associated with a type I interferon signature. *Nat. Genet.* 44: 1243–1248.
- Rice, G. I., Y. del Toro Duany, E. M. Jenkinson, G. M. A. Forte, B. H. Anderson, G. Ariaudo, B. Bader-Meunier, E. M. Baidam, R. Battini, M. W. Beresford, et al. 2014. Gain-of-function mutations in IFIH1 cause a spectrum of human disease phenotypes associated with upregulated type I interferon signaling. *Nat. Genet.* 46: 503–509.
- Yang, Y.-G., T. Lindahl, and D. E. Barnes. 2007. Trex1 exonuclease degrades ssDNA to prevent chronic checkpoint activation and autoimmune disease. *Cell* 131: 873–886.
- Stetson, D. B., J. S. Ko, T. Heidmann, and R. Medzhitov. 2008. Trex1 prevents cell-intrinsic initiation of autoimmunity. *Cell* 134: 587–598.
- Gall, A., P. Treuting, K. B. Elkon, Y.-M. Loo, M. Gale, Jr., G. N. Barber, and D. B. Stetson. 2012. Autoimmunity initiates in nonhematopoietic cells and progresses via lymphocytes in an interferon-dependent autoimmune disease. *Immunity* 36: 120–131.
- Lebon, P., J. Badoual, G. Ponsot, F. Goutières, F. Hémeury-Cukier, and J. Aicardi. 1988. Intrathecal synthesis of interferon-alpha in infants with progressive familial encephalopathy. *J. Neurol. Sci.* 84: 201–208.
- van Heteren, J. T., F. Rozenberg, E. Aronica, D. Troost, P. Lebon, and T. W. Kuijpers. 2008. Astrocytes produce interferon- $\alpha$  and CXCL10, but not IL-6 or CXCL8, in Aicardi-Goutières syndrome. *Glia* 56: 568–578.
- Takanohashi, A., M. Prust, J. Wang, H. Gordish-Dressman, M. Bloom, G. I. Rice, J. L. Schmidt, Y. J. Crow, P. Lebon, T. W. Kuijpers, et al. 2013. Elevation of proinflammatory cytokines in patients with Aicardi-Goutières syndrome. *Neurology* 80: 997–1002.
- Rice, G. I., G. M. A. Forte, M. Szykiewicz, D. S. Chase, A. Aeby, M. S. Abdel-Hamid, S. Ackroyd, R. Allcock, K. M. Bailey, U. Balottin, et al. 2013. Assessment of interferon-related biomarkers in Aicardi-Goutières syndrome associated with mutations in TREX1, RNASEH2A, RNASEH2B, RNASEH2C, SAMHD1, and ADAR: a case-control study. *Lancet Neurol.* 12: 1159–1169.
- Morita, M., G. Stamp, P. Robins, A. Dulic, I. Rosewell, G. Hrivnak, G. Daly, T. Lindahl, and D. E. Barnes. 2004. Gene-targeted mice lacking the Trex1 (DNase III) 3'→5' DNA exonuclease develop inflammatory myocarditis. *Mol. Cell. Biol.* 24: 6719–6727.
- Reijns, M. A. M., B. Rabe, R. E. Rigby, P. Mill, K. R. Astell, L. A. Lettice, S. Boyle, A. Leitch, M. Keighren, F. Kilanowski, et al. 2012. Enzymatic removal of ribonucleotides from DNA is essential for mammalian genome integrity and development. *Cell* 149: 1008–1022.
- Hiller, B., M. Achleitner, S. Glage, R. Naumann, R. Behrendt, and A. Roers. 2012. Mammalian RNase H2 removes ribonucleotides from DNA to maintain genome integrity. *J. Exp. Med.* 209: 1419–1426.
- Wang, Q., M. Miyakoda, W. Yang, J. Khillan, D. L. Stachura, M. J. Weiss, and K. Nishikura. 2004. Stress-induced apoptosis associated with null mutation of ADAR1 RNA editing deaminase gene. *J. Biol. Chem.* 279: 4952–4961.
- Behrendt, R., T. Schumann, A. Gerbaulet, L. A. Nguyen, N. Schubert, D. Alexopoulou, U. Berka, S. Lienenklaus, K. Peschke, K. Gibbert, et al. 2013. Mouse SAMHD1 has antiretroviral activity and suppresses a spontaneous cell-intrinsic antiviral response. *Cell Reports* 4: 689–696.
- Rehwinkel, J., J. Maelfait, A. Bridgeman, R. Rigby, B. Hayward, R. A. Liberatore, P. D. Bieniasz, G. J. Towers, L. F. Moita, Y. J. Crow, et al. 2013. SAMHD1-dependent retroviral control and escape in mice. *EMBO J.* 32: 2454–2462.
- Cuadrado, E., M. H. Jansen, J. Anink, L. De Filippis, A. L. Vescovi, C. Watts, E. Aronica, E. M. Hol, and T. W. Kuijpers. 2013. Chronic exposure of astrocytes to interferon- $\alpha$  reveals molecular changes related to Aicardi-Goutières syndrome. *Brain* 136: 245–258.
- Barth, P. G., A. Walter, and I. van Gelderen. 1999. Aicardi-Goutières syndrome: a genetic microangiopathy? *Acta Neuropathol.* 98: 212–216.
- Rasmussen, M., K. Skullerud, S. J. Bakke, P. Lebon, and F. L. Jahnsen. 2005. Cerebral thrombotic microangiopathy and antiphospholipid antibodies in Aicardi-Goutières syndrome—report of two sisters. *Neuropediatrics* 36: 40–44.
- Xin, B., S. Jones, E. G. Puffenberger, C. Hinze, A. Bright, H. Tan, A. Zhou, G. Wu, J. Vargus-Adams, D. Agamanolis, and H. Wang. 2011. Homozygous mutation in SAMHD1 gene causes cerebral vasculopathy and early onset stroke. *Proc. Natl. Acad. Sci. USA* 108: 5372–5377.
- Thiele, H., M. du Moulin, K. Barczyk, C. George, W. Schwindt, G. Nürnberg, M. Frosch, G. Kurlmann, J. Roth, P. Nürnberg, and F. Rutsch. 2010. Cerebral arterial stenoses and stroke: novel features of Aicardi-Goutières syndrome caused by the Arg164X mutation in SAMHD1 are associated with altered cytokine expression. *Hum. Mutat.* 31: E1836–E1850.
- Ramesh, V., B. Bernardi, A. Stafa, C. Garone, E. Franzoni, M. Abinun, P. Mitchell, D. Mitra, M. Friswell, J. Nelson, et al. 2010. Intracerebral large artery disease in Aicardi-Goutières syndrome implicates SAMHD1 in vascular homeostasis. *Dev. Med. Child Neurol.* 52: 725–732.
- Olivieri, I., M. Cattalini, D. Tonduti, R. La Piana, C. Uggetti, J. Galli, A. Meini, A. Tincani, D. Moratto, E. Fazzi, et al. 2013. Dysregulation of the immune system in Aicardi-Goutières syndrome: another example in a TREX1-mutated patient. *Lupus* 22: 1064–1069.
- Du Moulin, M., P. Nürnberg, Y. J. Crow, and F. Rutsch. 2011. Cerebral vasculopathy is a common feature in Aicardi-Goutières syndrome associated with SAMHD1 mutations. *Proc. Natl. Acad. Sci. USA* 108: E232; author reply E233.
- De Filippis, L., G. Lamorte, E. Y. Snyder, A. Malgaroli, and A. L. Vescovi. 2007. A novel, immortal, and multipotent human neural stem cell line generating functional neurons and oligodendrocytes. *Stem Cells* 25: 2312–2321.
- Smolders, J., K. G. Schuurman, M. E. van Strien, J. Melief, D. Hendrickx, E. M. Hol, C. van Eden, S. Luchetti, and I. Huitinga. 2013. Expression of vitamin D receptor and metabolizing enzymes in multiple sclerosis-affected brain tissue. *J. Neuropathol. Exp. Neurol.* 72: 91–105.
- Root, D. E., N. Hacohen, W. C. Hahn, E. S. Lander, and D. M. Sabatini. 2006. Genome-scale loss-of-function screening with a lentiviral RNAi library. *Nat. Methods* 3: 715–719.
- van Tijn, P., F. M. S. de Vrij, K. G. Schuurman, N. P. Dantuma, D. F. Fischer, F. W. van Leeuwen, and E. M. Hol. 2007. Dose-dependent inhibition of proteasome activity by a mutant ubiquitin associated with neurodegenerative disease. *J. Cell Sci.* 120: 1615–1623.
- Kamphuis, W., J. Middeldorp, L. Kooijman, J. A. Sluijs, E.-J. Kooi, M. Moeton, M. Freriks, M. R. Mizee, and E. M. Hol. 2014. Glial fibrillary acidic protein isoform expression in plaque related astrogliosis in Alzheimer's disease. *Neurobiol. Aging* 35: 492–510.
- Liang, C.-C., A. Y. Park, and J.-L. Guan. 2007. In vitro scratch assay: a convenient and inexpensive method for analysis of cell migration in vitro. *Nat. Protoc.* 2: 329–333.
- Navarro-Sobrinó, M., A. Rosell, M. Hernandez-Guillamon, A. Penalba, M. Ribó, J. Alvarez-Sabín, and J. Montaner. 2010. Mobilization, endothelial differentiation and functional capacity of endothelial progenitor cells after ischemic stroke. *Microvasc. Res.* 80: 317–323.
- Su, A. I., T. Wiltshire, S. Batalov, H. Lapp, K. A. Ching, D. Block, J. Zhang, R. Soden, M. Hayakawa, G. Kreiman, et al. 2004. A gene atlas of the mouse and human protein-encoding transcriptomes. *Proc. Natl. Acad. Sci. USA* 101: 6062–6067.
- Sestero, C. M., D. J. McGuire, P. De Sarno, E. C. Brantley, G. Soldevila, R. C. Axtell, and C. Raman. 2012. CD5-dependent CK2 activation pathway regulates threshold for T cell energy. *J. Immunol.* 189: 2918–2930.
- Auerbach, R., R. Lewis, B. Shinnars, L. Kubai, and N. Akhtar. 2003. Angiogenesis assays: a critical overview. *Clin. Chem.* 49: 32–40.
- Izzotti, A., M. Longobardi, C. Cartiglia, F. Anzuini, P. Arrigo, E. Fazzi, S. Orcesi, R. L. Piana, and A. Pulliero. 2012. Different mutations in three prime repair exonuclease 1 and ribonuclease H2 genes affect clinical features in Aicardi-Goutières syndrome. *J. Child Neurol.* 27: 51–60.
- Pereira-Lopes, S., T. Celhar, G. Sans-Fons, M. Serra, A.-M. Fairhurst, J. Lloberas, and A. Celada. 2013. The exonuclease Trex1 restrains macrophage proinflammatory activation. *J. Immunol.* 191: 6128–6135.
- Franzolin, E., G. Pontarin, C. Rampazzo, C. Miazzi, P. Ferraro, E. Palumbo, P. Reichard, and V. Bianchi. 2013. The deoxynucleotide triphosphohydrolase SAMHD1 is a major regulator of DNA precursor pools in mammalian cells. *Proc. Natl. Acad. Sci. USA* 110: 14272–14277.

42. Kretschmer, S., C. Wolf, N. Konig, W. Staroske, J. Guck, M. Hausler, H. Luksch, L. A. Nguyen, B. Kim, D. Alexopoulou, et al. 2015. SAMHD1 prevents autoimmunity by maintaining genome stability. *Ann. Rheum. Dis.* 74: e17.
43. Li, Z., K. C. Wolff, and C. E. Samuel. 2010. RNA adenosine deaminase ADAR1 deficiency leads to increased activation of protein kinase PKR and reduced vesicular stomatitis virus growth following interferon treatment. *Virology* 396: 316–322.
44. Kirkwood, J. 2002. Cancer immunotherapy: the interferon-alpha experience. *Semin. Oncol.* 29(3, Suppl. 7):18–26.
45. Lebon, P., J. F. Meritet, A. Krivine, and F. Rozenberg. 2002. Interferon and Aicardi-Goutières syndrome. *Eur. J. Paediatr. Neurol.* 6(Suppl. A): A47–A53; discussion A55–A58, A77–A86.
46. Izzotti, A., E. Fazzi, S. Orcesi, C. Cartiglia, M. Longobardi, V. Capra, P. Lebon, A. Cama, A. Pulliero, R. La Piana, and G. Lanzi. 2008. Brain damage as detected by cDNA-microarray in the spinal fluid of patients with Aicardi-Goutières syndrome. *Neurology* 71: 610–612.
47. Yang, S.-Z., L.-M. Zhang, Y.-L. Huang, and F.-Y. Sun. 2003. Distribution of Flk-1 and Flt-1 receptors in neonatal and adult rat brains. *Anat. Rec. A Discov. Mol. Cell. Evol. Biol.* 274: 851–856.
48. Noyce, R. S., S. E. Collins, and K. L. Mossman. 2006. Identification of a novel pathway essential for the immediate-early, interferon-independent antiviral response to enveloped virions. *J. Virol.* 80: 226–235.
49. Hasan, M., J. Koch, D. Rakheja, A. K. Pattnaik, J. Brugarolas, I. Dozmorov, B. Levine, E. K. Wakeland, M. A. Lee-Kirsch, and N. Yan. 2013. Trex1 regulates lysosomal biogenesis and interferon-independent activation of antiviral genes. *Nat. Immunol.* 14: 61–71.